Thin Solid Films 518 (2010) 3428–3431

Contents lists available at ScienceDirect

Thin Solid Films

journal homepage: www.elsevier.com/locate/tsf

Hole transport properties of p-type polycrystalline ZnO film using a dual-acceptor doping method with lithium and nitrogen

X.H. Wang [a,b,*], B. Yao [b], C.X. Cong [b], Z.P. Wei [b], D.Z. Shen [b], Z.Z. Zhang [b], B.H. Li [b], Y.M. Lu [b], D.X. Zhao [b], J.Y. Zhang [b], X.W. Fan [b]

[a] School of Mechanical Engineering, Shanghai Dianji University, Shanghai 200240, PR China
[b] Key Laboratory of Excited State Processes, Changchun Institute of Optics, Fine Mechanics and Physics, Chinese Academy of Sciences, Changchun,130033, PR China

ARTICLE INFO

Article history:
Received 30 March 2008
Received in revised form 27 November 2009
Accepted 1 December 2009
Available online 6 December 2009

Keywords:
Polycrystalline film
Transport properties
P-type ZnO
Hall-effect measurement

ABSTRACT

Hole transport properties of p-type polycrystalline ZnO film using a dual-acceptor doping method with lithium and nitrogen (denoted as ZnO:(Li, N)) were investigated by the temperature-dependent Hall-effect measurements. The hole mobility of the ZnO:(Li, N) firstly increases with increasing temperature from 85 to 140 K, and then decreases from 140 to 300 K. The comparison of experimental results and theoretical models shows that the mobility at temperature below 140 K is mainly affected by the grain boundary scattering, whereas the hole mobility above 140 K is dominated by mixed scatterings, involving lattice vibration, dislocation, and ionized impurity.

1. Introduction

Wurtzite ZnO is a II–VI compound semiconductor with many excellent physical properties, such as high optical gain of 300 cm^{-1} and a large excitonic binding energy of 60 meV [1] at room temperature, which is much larger than those of ZnSe (22 meV) and GaN (25 meV) [2]. In this regard, ZnO is a promising candidate for ultraviolet light-emitting diodes, laser diodes, and photodetectors [3]. As the performance of these ZnO-based optoelectronic devices strongly relies on the quality of films, synthesis of high-quality n- and p-type ZnO films is crucial. Due to the native properties of ZnO films, n-type ZnO could be relatively easily produced, even without any intentional doping. However, fabrication of a reproducible and high-quality p-type ZnO is very difficult due to self-compensating effect, deep acceptor level, and low solubility of acceptor dopants [4,5].

In recent years, many research groups have fabricated p-type ZnO films by introducing various of dopants like N [6,7], P [8,9], As [10–12], and Sb [13]. However, the hole mobility of these films has not reached the theoretical value of 70 $cm^2 v^{-1} s^{-1}$ [14], and the physical cause of such low mobility is still not well understood. Sun et al. [15] investigated the hole transport properties of the N-doped p-type ZnO films with highly preferential orientation in the (0 0 2) direction and demonstrated that the inhomogeneous microstructure in p-type ZnO films plays an important role in determining the hole mobility. Steinhauser et al. [16] argued that the transport is dependent on the doping level in ZnO film. For the lightly doped films, the dominant scattering process is grain scattering, whereas in the case of heavily doped films, the intragrain ionized impurity is mainly responsible for the scattering.

Recently, we have developed a reliable and reproducible method to grow p-type polycrystalline ZnO film doped with lithium and nitrogen, and discussed the p-type formation mechanism [17]. In the present work, the hole transport properties of the p-type polycrystalline ZnO are investigated by temperature-dependent Hall-effect measurement from 85 to 300 K and the transport mechanisms are discussed in detail.

2. Experiments

A Zn–Li alloy with nominal 2 at.% Li was prepared by arc-melting technique. X-ray diffraction (XRD) measurement confirmed that Li has incorporated into the Zn–Li alloy by substituting for Zn, and the Li content was estimated to be about 1.63 at.% by using the XRD data and Vegard formula [18]. A 500 nm thick Li-doped Zn_3N_2 film was grown on a *c*-plane Al_2O_3 substrate at 300 K by RF-magnetron sputtering process with the target of Zn–Li alloy and the working gas of nitrogen

* Corresponding author. School of Mechanical Engineering, Shanghai Dianji University, Shanghai 200240, PR China. Tel.: +86 21 64300980 3010.
E-mail address: xianghuwang@yahoo.com.cn (X.H. Wang).

0040-6090/$ – see front matter © 2009 Elsevier B.V. All rights reserved.
doi:10.1016/j.tsf.2009.12.007

(pressure = 1.0 Pa). Before deposition, the substrate was treated with ethanol in an ultrasonic bath to remove surface contaminations and etched in hot (160 °C) H_2SO_4:H_3PO_4 (3:1) solution for 10 min. The high-purity nitrogen gas was used to dry the substrate which was rinsed in de-ionized water (18.2 MΩ cm). The as-grown film was annealed in flowing O_2 gas at 600 °C for 30 min. Crystal structure characterization was performed by using a Rigaku O/max-RA X-ray diffractometer with Cu Kα_1 radiation ($\lambda = 0.15418$ nm). The temperature-dependent Hall-effect was measured by Lakershore HMS 7707 in a temperature range of 85 to 300 K and the contacts were made by Au/Ni. Before the measurements of the electrical properties of the sample, the ohmic contact was confirmed by measuring the I–V curve of the sample.

3. Results and discussion

Fig. 1(a) and (b) show XRD patterns of the as-grown Li-doped Zn_3N_2 sample and the sample annealed for 30 min at 600 °C in flowing O_2 gas, respectively. A preferential orientation of (400) diffraction is clearly present (Fig. 1(a)). After annealing, the Li-doped Zn_3N_2 is transformed into wurtzite ZnO:(Li, N) film. Three diffraction peaks are identified as diffractions of (100), (002) and (101) planes of the ZnO:(Li, N), as shown in Fig. 1(b), indicating that the ZnO:(Li, N) is a polycrystalline film. Mean grain size of the ZnO:(Li, N) was calculated to be 88 nm ($L = 88$ nm) by using XRD data and Scherrer's formula,

$$d = \frac{0.9\lambda}{B\cos}\theta_B \tag{1}$$

where λ, θ_B, and B are the X-ray wavelength (1.5418 Å), Bragg diffraction angle, and full-width at half-maximum, respectively.

The temperature-dependent Hall measurements were carried out from 85 to 300 K. Fig. 2(a) shows the variation of the hole concentration versus temperature. It is found that the hole concentration increases with temperature from 85 to 300 K. The temperature dependence of the hole mobility is shown in Fig. 2(b). The hole mobility firstly increases with increasing temperature from 85 to 140 K, and then decreases with further increasing temperature to 300 K, implying that the hole mobility might be dominated by different scattering mechanisms in the different temperature regions.

In order to better understand the hole transport properties of ZnO:(Li, N), we investigate the scattering mechanisms in different temperature regions. The main scattering mechanisms in a single-crystal semiconductor include the ionized impurity scattering (μ_i), acoustic-mode deformation potential scattering (μ_{as}), acoustic-mode piezoelectric potential scattering (μ_{pz}), and polar optical phonon scattering (μ_{pop}). Sun et al. calculated the variation of the hole mobility with temperature based on these four scattering mechanisms in ZnO film [15], and the calculated value of hole mobility at low temperatures is two orders of magnitude larger than the experimental value of hole mobility from the temperature-dependent Hall measurement in ZnO:(Li,N) film, as shown in Fig. 2(b). The large discrepancy manifests that the four types of scattering mentioned above are not applicable for the p-type polycrystalline ZnO:(Li,N) in the temperature region from 85 to 140 K.

Note that the ZnO:(Li,N) is a polycrystalline film with mean grain size of 88 nm, indicating that the grain boundary scattering (μ_{grain}) cannot be excluded in the present ZnO:(Li,N) film. The mobility dominated by grain boundary scattering can be expressed as [19]:

$$\mu_{grain} = \frac{Le}{(2\pi m_p{}^* k_B)^{1/2}} T^{-1/2} \exp\left(-\frac{E_b}{k_B T}\right) \tag{2}$$

where L is the grain size, E_b is the barrier height across the grain boundary, k_B is Boltzmann constant and m_p is the effective mass of the hole. In Eq. (2), the effective hole mass is assumed to be 0.64 m_0 (m_0 is the free electron mass) [20]. From Eq. (2), the following expression can be yielded,

$$\ln \mu_{grain} T^{1/2} = \ln \frac{Le}{(2\pi m_p k_B)^{1/2}} - \frac{E_b}{k_B} T^{-1} \tag{3}$$

In Eq. (3), the value of $\ln \frac{Le}{(2\pi m_p k_B)^{1/2}}$ is a constant, therefore, the variation of $\ln(\mu_{grain} T^{1/2})$ versus T^{-1} should behave a straight line with a minus slope. Fig. 3 shows the plot of $\ln(\mu T^{1/2})$ versus T^{-1} from 85 to 140 K for ZnO:(Li,N) film, which corresponds to Eq. (3) very well, implying that the mobility is mainly affected by grain boundary scattering in the temperature range of 85–140 K. Moreover, the fitting parameters of E_b and L can be obtained as 6.78 meV and 90 nm, respectively. The fitting value of L is closed to 88 nm calculated by XRD, which also manifests that the hole transport is dominated by the grain boundary scattering.

According to grain boundary scattering mechanisms, the conductivity (σ) depends on the grain size L, the carrier concentration N in crystallite, and the density of trapping states (Q_t) locating at energy E_t with respect to the intrinsic Fermi level. In a real polycrystalline material, the

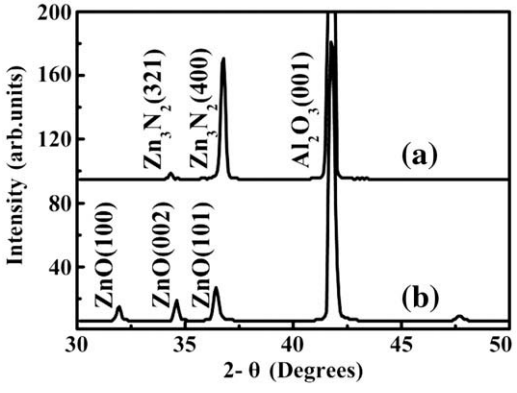

Fig. 1. XRD patterns of as-sputtered Li-doped Zn_3N_2 sample (a), and the ZnO:(Li,N) sample produced by annealing the Zn_3N_2 at 600 °C in O_2 ambient (b).

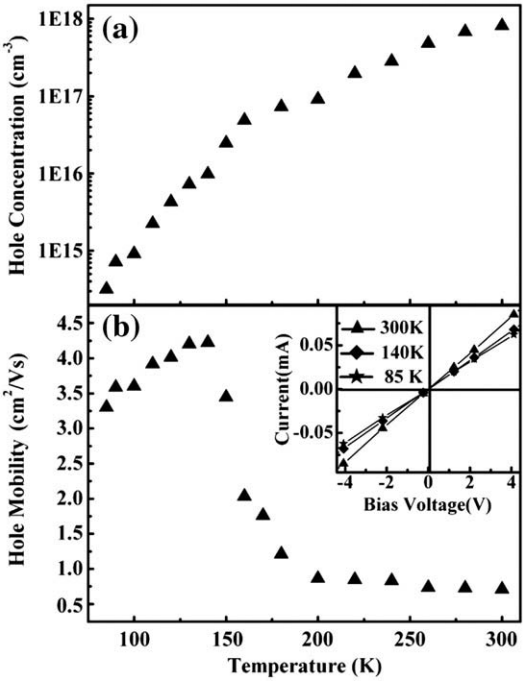

Fig. 2. Temperature dependence of the hole concentration (a), and the hole mobility (b).

crystallites have a distribution of sizes and irregular shapes. To simplify the model, the p-type polycrystalline ZnO:(Li,N) film is assumed to be composed of identical crystallites having the grain size of L cm. For a given crystallite size, there exist two possible conditions depending on the hole concentration in crystallite: (a) $LN<Q_t$, and (b) $LN>Q_t$. For $LN<Q_t$, the crystallite is completely depleted of holes and the traps are partially filled, so the conductivity (σ) can be expressed as follows [19],

$$\sigma = \frac{2\pi e^2 L^2 m_p^* N_p k_B T}{h^3 (Q_t - LN_p)} \exp\left(-\frac{E_a}{k_B T}\right) \tag{4}$$

where $E_a = E_g/2 - E_t$ is the activation energy, E_g is the band gap, and N_p is the hole concentration. For $LN>Q_t$, the crystallite is partially depleted of holes and the traps are completely filled. In this case, the conductivity (σ) has two limiting cases depending on the location of trap states (E_t) with respective to Fermi level (E_f): (1) when the trap states are below the Fermi level, i.e., $E_f - (E_t + E_b) \geq k_B T$, σ is given by

$$\sigma = \frac{e^2 L N_p}{(2\pi m_p^* k_B T)^{1/2}} \exp\left(-\frac{E_a}{k_B T}\right) \tag{5}$$

where the activation energy E_a is equal to E_b; and (2) when the trap states are above the Fermi level, i.e., $(E_t + E_b) - E_f \geq k_B T$, σ is given by

$$\sigma = \frac{4eL}{Q_t} \left(\frac{\varepsilon E_b k_B^5}{\pi m_p^* N_p}\right)^{1/2} \left(\frac{2\pi m_p^*}{h^2}\right) T^{5/2} \exp\left(-\frac{E_a}{k_B T}\right) \tag{6}$$

where the activation energy E_a is equal to $E_g/2 - E_t$.

In order to confirm the grain boundary scattering mechanism in the low-temperature region from 85 to 140 K, the variation of $\ln(\sigma T^{1/2})$ versus T^{-1} behavior was also calculated according to Eqs. (4)–(6). Fig. 4 shows $\ln(\sigma T^{1/2})$ as a function of T^{-1} and we found that only the calculated data based on Eq. (5) are consistent with the experimental values (not shown for the case of Eqs. (4) and (6)). The results further confirm that the hole transport in the low-temperature region is dominated by grain boundary scattering mechanism and the trap states are below the Fermi level. From Fig. 4, it can be clearly seen that the variation of $\ln(\sigma T^{1/2})$ versus T^{-1} shows a straight line with a minus slope. However, the activation energy E_a is not equal to the value of slope. What causes the large difference? From Eq. (5), the following expression can be yielded,

$$\ln \sigma T^{1/2} = \ln \frac{e^2 L N_p}{(2\pi m_p^* k_B T)^{1/2}} - \frac{E_a}{k_B T} \tag{7}$$

In Eq. (7), $\ln \frac{e^2 L N_p}{(2\pi m_p^* k_B T)^{1/2}}$ is not a constant because the hole concentration N_p is a function of T. Therefore, "Non-Linear Cure Fit" is used and the E_a is 6.78 meV from the fitting results, which is the same as E_b obtained by fitting the data according to Eq. (3).

Next, the hole transport properties were investigated in the temperature region from 140 to 300 K. As Fig. 2(b) shows, the hole mobility in the temperature region (140–300 K) decreases with the increase of temperature. In our work, the variation of mobility with temperature due to lattice vibration scattering was calculated by using the formula: $\mu_{latt}^{-1} = \mu_{pop}^{-1} + \mu_{as}^{-1} + \mu_{pz}^{-1}$, as shown by the dashed line in Fig. 5. The parameters related to ZnO used in the calculation are given in the literature [21]. It is seen that the variation of the measured mobility versus temperature is close to the calculated values, however, there is a little discrepancy between the measured mobility and calculated value, implying that the mobility is mainly affected by lattice vibration scattering while other types of scattering also co-exist. Considering the polycrystalline property of the film, the effect of grain boundary might play some roles. However, when we used the formula: $\mu^{-1} = \mu_{grain}^{-1} + \mu_{latt}^{-1}$ to calculate the mobility, we found that the discrepancy between the measured mobility and calculated value was magnified, indicating that the grain boundary scattering mechanism has not much effect on the mobility in the temperature region from 140 to 300 K. Xiao et al. [21] investigated the hole transport properties of p-type polycrystalline ZnO film doped by nitrogen, and they proposed that the dislocation scattering (μ_{dis}) has an effect on hole transport properties of p-type polycrystalline ZnO film grown on a large mismatched substrate. Owing to the lattice mismatch between ZnO and sapphire (18%) [22], the dislocation scattering should be important in the film. Therefore, a mixed scattering process must be included, which are acoustic-mode deformation potential scattering, acoustic-mode piezoelectric potential scattering, polar optical phonon scattering, and dislocation scattering. The total mobility (μ_{total}) can be written as:

$$\mu_{total}^{-1} = \mu_{latt}^{-1} + \mu_{dis}^{-1} \tag{8}$$

Using Eq. (8) to calculate the values of hole mobility, we find that the discrepancy between the Hall-effect measured mobility and calculated value is reduced, indicating that the dislocation scattering has also effect on the hole mobility. Moreover, as proposed by Steinhauser et al. [16], the ionized impurity scattering also has to be considered. When the ionized impurity scattering is also included into the Eq. (8), it is noted that the calculated values are much closer to the measured values. The best fitting parameters for the ionized acceptor impurity concentration ($N_i \sim 10^{19}\ \mathrm{cm}^{-3}$) and the dislocation density ($N_{dis} \sim 7.9 \times 10^{11}\ \mathrm{cm}^{-2}$) were obtained by using the formula: $\mu_{total}^{-1} = \mu_{latt}^{-1} + \mu_{dis}^{-1} + \mu_i^{-1}$ to fit the experimental mobility data, as shown in Fig. 5. These values are reasonable, indicating that besides the main scattering mechanism of lattice vibration scattering, the dislocation and the ionized impurity

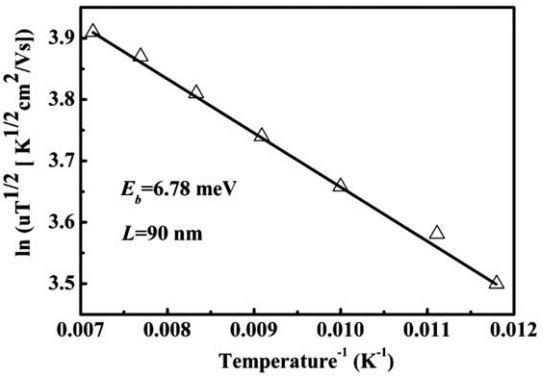

Fig. 3. The variation of $\ln(\mu T^{1/2})$ versus T^{-1} from 85 to 140 K. The solid line represents the fitting curve according Eq. (3).

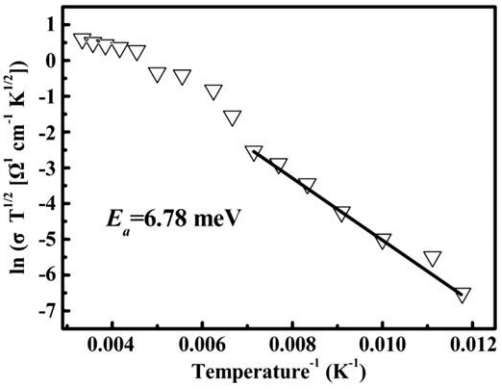

Fig. 4. The plot of $\ln(\sigma T^{1/2})$ versus T^{-1} from 85 to 140 K. The solid line is the calculated data using Eq. (5).

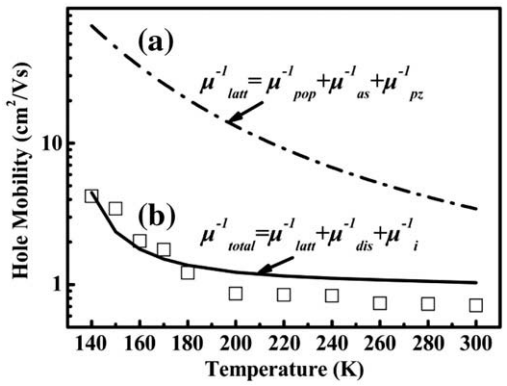

Fig. 5. The hole mobility of ZnO:(Li,N) film as a function of temperature from 140 to 300 K. The dashed curve is the calculated data based on the lattice vibration scattering mechanism and the fitting curve according to the lattice vibration, dislocation, and ionized impurity scattering mechanisms.

scatterings have also great effects on hole transport properties in the higher temperature region from 140 to 300 K.

Based on the above analysis, the hole mobility properties in the p-type polycrystalline ZnO:(Li,N) can be clarified that the grain boundary scattering is dominant in the temperature ranging from 85 to 140 K because most of the hole carrier cannot exceed the potential energy of grain boundary (6.78 meV) due to the lower energy of hole carrier at low temperature. Meanwhile, though a small amount of acceptor impurity might be ionized, the majority is still electrically neutral, due to the lower thermal energy in the low-temperature region. Also, the hole concentration and the probability that the hole takes up the dislocation are low, which could dramatically weaken the effects of the ionized impurity and dislocation scatterings on the hole mobility. When the temperature is above 140 K, the hole carrier has higher thermal energy, and most of them are over the potential energy of grain boundary. Thus, the grain boundary scattering becomes a minor contributor. However, the amount of the ionized acceptor impurities and the probability that the hole takes up the dislocation will increase. Consequently, their effects become more dominant besides the lattice vibration scattering process in the higher temperature ranging from 140 to 300 K.

4. Conclusions

Hole transport properties of p-type polycrystalline ZnO:(Li,N) were investigated by the temperature-dependent Hall-effect measurements. The mobility increases with increasing temperature from 85 to 140 K, and then decreases from 140 to 300 K. The good agreement between the experimental data and theoretical fitting reveals that the mobility is dominated by the grain boundary scattering in the lower temperature region while the mixed scattering processes including the lattice vibration, dislocation and ionized impurity scattering are responsible in the higher temperature range.

Acknowledgements

This work was supported by the National Natural Science Foundation of China under contract 10804071, Shanghai Municipal Education Commission Project under contract sdj08013, Shanghai Dianji University Project under contracts 08C409 and 08A128 (Matched Foundation), the program of CAS Hundred Talents, Key Projects of the National Natural Science Foundation of China (Grant No. 60336020).

References

[1] M. Kawasaki, A. Ohtomo, I. Ohkuho, H. Koinuma, Z.K. Tang, P. Yu, G.K.L. Wong, B.P. Zhang, Y. Segawa, Mater. Sci. Eng. B 56 (1998) 239.
[2] S.J. Yeon, V.Oleg Kononenko, C. Won-Kook, Solid State Commun. 137 (2006) 474.
[3] A. Krtschil, A. Dadgar, N. Oleynik, J. Blasing, A. Diez, A. Krost, Appl. Phys. Lett. 87 (2005) 262105.
[4] S.B. Zhang, S.H. Wei, A. Zunger, Phys. Rev. B 63 (2001) 075205.
[5] E.C. Lee, Y.S. Kim, Y.G. Jin, K.J. Chang, Phys. Rev. B 64 (2001) 085120.
[6] H.W. Liang, Y.M. Lu, D.Z. Shen, Y.C. Liu, J.F. Yan, C.X. Shan, B.H. Li, Z.Z. Zhang, J.Y. Zhang, X.W. Fan, Phys. Status Solidi A 202 (2005) 1060.
[7] D.C. Look, D.C. Reynolds, C.W. Litton, R.L. Jones, D.B. Eason, G. Cantwell, Appl. Phys. Lett. 81 (2002) 1830.
[8] D.K. Hwang, H.S. Kim, J.H. Lim, J.Y. Oh, J.H. Yang, S.J. Park, K.K. Kim, D.C. Look, Y.S. Park, Appl. Phys. Lett. 86 (2005) 151917.
[9] K.K. Kim, H.S. Kim, D.K. Hwang, J.H. Lim, S.J. Park, Appl. Phys. Lett. 83 (2003) 63.
[10] Y.R. Ryu, T.S. Lee, H.W. White, Appl. Phys. Lett. 83 (2003) 87.
[11] D.C. Look, G.M. Renlund, R.H. Burgener, J.R. Sizelove, Appl. Phys. Lett. 85 (2004) 5269.
[12] V. Vaithianathan, B.T. Lee, S.S. Kim, Appl. Phys. Lett. 86 (2005) 062101.
[13] F.X. Xiu, Z. Yang, L.J. Mandalapu, D.T. Zhao, J.L. Liu, W.P. Beyermann, Appl. Phys. Lett. 87 (2005) 152101.
[14] T. Makino, A. Ohtomo, A. Tsukazaki, M. Kawasaki, H. Koinuma, Jpn. J. Appl. Phys. 45 (2006) 6346.
[15] J.W. Sun, Y.M. Lu, Y.C. Liu, D.Z. Shen, Z.Z. Zhang, B.H. Li, J.Y. Zhang, B. Yao, D.X. Zhao, X.W. Fan, Appl. Phys. Lett. 89 (2006) 232101.
[16] J. Steinhauser, S. Faÿ, N. Oliveira, E. Vallat-Sauvain, C. Ballif, Appl. Phys. Lett. 90 (2007) 142107.
[17] X.H. Wang, B. Yao, Z.P. Wei, D.Z. Sheng, Z.Z. Zhang, B.H. Li, Y.M. Lu, D.X. Zhao, J.Y. Zhang, X.W. Fan, L.X. Guan, C.X. Cong, J. Phys. D: Appl. Phys. 39 (2006) 4568.
[18] X.H. Wang, B. Yao, Z.Z. Zhang, B.H. Li, Z.P. Wei, D.Z. Shen, Y.M. Lu, X.W. Fan, Semicond. Sci. Technol. 21 (2006) 494.
[19] J.Y.W. Seto, J. Appl. Phys. 46 (1975) 5247.
[20] D.C. Look, Semicond. Sci. Technol. 20 (2005) S55.
[21] Z.Y. Xiao, Y.C. Liu, B.H. Li, J.Y. Zhang, Y.M. Lu, D.Z. Shen, X.W. Fan, Semicond. Sci. Technol. 21 (2006) 1522.
[22] P. Zu, Z.K. Tang, G.K.L. Wong, M. Kawasaki, A. Ohtomo, H. Koinuma, Y. Segawa, Solid State Commun. 103 (1997) 459.